Prilog 18

SimTerm 2019

Energy – Efficiency – Ecology

PROCEEDINGS

19th International Conference on
Thermal Science and Engineering of Serbia

Sokobanja
October 22-25
2019

Prilog 18

SimTerm 2019

PROCEEDINGS

19th International Conference on Thermal Science and Engineering of Serbia

Sokobanja, Serbia, October 22 – 25, 2019

University of Niš, Faculty of Mechanical Engineering in Niš, Department of Thermal Engineering and Society of Thermal Engineers of Serbia

ISBN 978-6055-124-7

Publisher: Faculty of Mechanical Engineering in Niš

2019

19th International Conference on **Thermal Science and Engineering of Serbia**

under the title

Energy – Ecology – Efficiency

is organized by

UNIVERSITY OF NIŠ, FACULTY OF MECHANICAL ENGINEERING IN NIŠ, DEPARTMENT OF THERMAL ENGINEERING and

SOCIETY OF THERMAL ENGINEERS OF SERBIA

under the patronage of the

GOVERNMENT OF THE REPUBLIC OF SERBIA

MINISTRY OF EDUCATION, SCIENCE AND TECHNOLOGICAL DEVELOPMENT

CITY OF NIŠ

and supported by donors and sponsors

ELECTRIC POWER INDUSTRY OF SERBIA

OVEX

ICNT

NIGOS ELEKTRONIK

WILO

HERZ

SD CRVENI KRST NIŠ

Prilog 18

GOVERNMENT OF THE REPUBLIC OF SERBIA

MINISTRY OF EDUCATION, SCIENCE AND TECHNOLOGICAL DEVELOPMENT

MINISTRY OF MINING AND ENERGY

International Scientific Committee

Dr Jordan Hristov, University of Chemical Technology and Metallurgy, Department of Chemical Engineering, Sofia, Bulgaria
Dr Gligor Kanevče, Macedonian Academy of Sciences and Arts, Skopje, North Macedonia
Dr Mikhail Shatrov, Moscow Automobile and Road Construction State Technical University, Moscow, Russia
Dr Zvonimir Guzović, University of Zagreb, Faculty of Mechanical Engineering and Naval Architecture, Zagreb, Croatia
Dr Igor Vušanović, University of Montenegro, The Faculty of Mechanical Engineering, Podgorica, Montenegro
Dr Anna Stoppato, University of Padova, Department of Industrial Engineering, Padova, Italy
Dr Slavtcho G. Slavtchev, Institute of Mechanics, Bulgarian Academy of Sciences, Sofia, Bulgaria
Dr Agis Papadoupoulos, Aristotle University Thessaloniki, Department of Mechanical Engineering, Thessaloniki, Greece
Dr Joseph N. Moore, University of Utah, Energy & Geoscience Institute, Salt Lake City, USA
Dr Konstantinos Papakostas, Aristotle University Thessaloniki, Department of Mechanical Engineering, Thessaloniki, Greece
Dr Sophia Natalia Boemi, Aristotle University Thessaloniki, Department of Mechanical Engineering, Thessaloniki, Greece
Dr Petar Novak, University of Novo mesto, Faculty of mechanical engineering, Novo mesto, Slovenia
Dr Iliya Iliyev, University of Ruse,Department of Thermotechnics, Hydraulic and Ecology, Ruse, Bulgaria
Dr Dušan Golubović, University of East Sarajevo, Faculty of Mechanical Engineering, Sarajevo, Republic of Srpska, Bosnia and Herzegovina
Dr Ljubica Kanevče, St. Kliment Ohridski University, Faculty of Technical Sciences, Bitola, North Macedonia
Dr Petar Gvero, University of Banja Luka, Faculty of Mechanical Engineering, Banja Luka, Republic of Srpska, Bosnia and Herzegovina
Dr Maria Ichim, Institute for Bioengineering, Biotechnology and Environmental Protection, Bucharest, Romania
Dr Vesna Barišić, Sumitomo SHI FW, Espoo, Finland
Dr Dečan Ivanović, University of Montenegro, The Faculty of Mechanical Engineering, Podgorica, Montenegro
Dr Friedrich Dinkelacker, Leibniz University Hannover, Faculty of Electrical Engineering and Computer Science, Hannover, Germany
Dr Risto Filkoski, Ss. Cyril and Methodius University, Faculty of Mechanical Engineering, Skopje, North Macedonia
Dr Tetyana Morozyuk, Technical University Berlin, Institute for Energy Engineering, Berlin, Germany
Dr Zlatan Car, University of Rijeka, Faculty of Engineering, Rijeka, Croatia
Dr Darko Knežević, University of Banja Luka, Faculty of Mechanical Engineering, Republic of Srpska, Banja Luka, Bosnia and Herzegovina
Dr Gyula Gróf, Department of Energy Engineering Hungary, Budapest, Hungary
Dr Zdravko Milovanović, University of Banja Luka, Faculty of Mechanical Engineering, Banja Luka, Republic of Srpska, Bosnia and Herzegovina
Dr Breda Kegl, University of Maribor, Faculty of mechanical engineering, Maribor, Slovenia
Dr Vladimir G. Tuponogov, Ural Federal University named after the first President of Russia B. N. Yeltsin, Ekaterinburg, Russia
Dr Vladimir Mijakovski, St. Kliment Ohridski University, Faculty of Technical Sciences, Bitola, North Macedonia
Dr Violeta Rasheva, University of Food Technology Plovdiv, Department of Industrial Thermal Engineering, Plovdiv, Bulgaria
Dr Oleh Onysko, Ivano-Frankivsk National Technical University of Oil and Gas, Ivano-Frankivsk, Ukraine
Dr Lubomir Dimitrov, Technical University of Sofia, Sofia, Bulgaria
Dr Birol Kilkis, Turkish Society of HVAC & Sanitary Engineers, Ankara, Turkiye

Program Committee

Dr Mladen Stojiljković, University of Niš, Faculty of Mechanical Engineering, Niš, Serbia
Dr Milan Radovanović, University of Belgrade, Faculty of Mechanical Engineering, Belgrade, Serbia
Dr Simeon Oka, University of Belgrade, Vinča Institute of Nuclear Sciences, Belgrade, Serbia
Dr Miloš Banjac, University of Belgrade, Faculty of Mechanical Engineering, Belgrade, Serbia
Dr Dragoslava Stojiljković, University of Belgrade, Faculty of Mechanical Engineering, Belgrade, Serbia
Dr Predrag Stefanović, University of Belgrade, Vinča Institute of Nuclear Sciences, Belgrade, Serbia
Dr Miodrag Mesarović, Serbian World Energy Council member committee, Belgrade, Serbia
Dr Dušan Gvozdenac, University of Novi Sad, Faculty of Technical Sciences, Novi Sad, Serbia
Dr Milun Babić, University of Kragujevac, Faculty of Engineering, Kragujevac, Serbia
Dr Vladan Karamarković, University of Kragujevac, Faculty of Mechanical and Civil Engineering, Kragujevac, Serbia
Dr Maja Todorović, University of Belgrade, Faculty of Mechanical Engineering, Belgrade, Serbia
Dr Dragoljub Živković, University of Niš, Faculty of Mechanical Engineering, Niš, Serbia
Dr Dragan Pantić, University of Niš, Faculty of Electronic Engineering, Niš, Serbia
Dr Velimir Strefanović, University of Niš, Faculty of Mechanical Engineering, Niš, Serbia
Dr Borislav Grubor, University of Belgrade, Vinča Institute of Nuclear Sciences, Belgrade, Serbia
Dr Valentino Stojkovski, Ss. Cyril and Methodius University, Faculty of Mechanical Engineering, Skopje, North Macedonia
Dr Maja Đurović Petrović, University of Belgrade, Faculty of Mechanical Engineering, Belgrade, Serbia
Dr Mirjana Laković-Paunović, University of Niš, Faculty of Mechanical Engineering, Niš, Serbia
Dr Mića Vukić, University of Niš, Faculty of Mechanical Engineering, Niš, Serbia
Dr Vukman Bakić, University of Belgrade, Vinča Institute of Nuclear Sciences, Belgrade, Serbia
Dr Dejan Ivezić, University of Belgrade, Faculty of Mining and Geology, Belgrade, Serbia
Dr Uroš Karadžić, University of Montenegro, The Faculty of Mechanical Engineering, Podgorica, Montenegro
Dr Jelena Janevski, University of Niš, Faculty of Mechanical Engineering, Niš, Serbia
Dr Predrag Živković, University of Niš, Faculty of Mechanical Engineering, Niš, Serbia

Honorary Committee

Dr Mladen Stojiljković, University of Niš, Faculty of Mechanical Engineering, Niš, Serbia
Dr Nenad T. Pavlović, University of Niš, Faculty of Mechanical Engineering, Niš, Serbia
Dr Vlastimir Nikolić, University of Niš, Faculty of Mechanical Engineering, Niš, Serbia
Dr Slobodan Laković, University of Niš, Faculty of Mechanical Engineering, Niš, Serbia
Dr Nenad Radojković, University of Niš, Faculty of Mechanical Engineering, Niš, Serbia
Dr Gradimir Ilić, University of Niš, Faculty of Mechanical Engineering, Niš, Serbia
Dr Zoran Boričić, University of Niš, Faculty of Mechanical Engineering, Niš, Serbia
Dr Žarko Stevanović, University of Belgrade, Vinča Institute of Nuclear Sciences, Belgrade, Serbia

Organizing Committee

Dr Mirjana Laković-Paunović, University of Niš, Faculty of Mechanical Engineering, Niš, Serbia
Dr Dejan Mitrović, University of Niš, Faculty of Mechanical Engineering, Niš, Serbia
Dr Mirko Stojiljković, University of Niš, Faculty of Mechanical Engineering, Niš, Serbia
Dr Marko Ignjatović, University of Niš, Faculty of Mechanical Engineering, Niš, Serbia
Dr Branislav Stojanović, University of Niš, Faculty of Mechanical Engineering, Niš, Serbia
Dr Mića Vukić, University of Niš, Faculty of Mechanical Engineering, Niš, Serbia
Dr Jelena Janevski, University of Niš, Faculty of Mechanical Engineering, Niš, Serbia
Dr Goran Vučković, University of Niš, Faculty of Mechanical Engineering, Niš, Serbia
Dr Predrag Živković, University of Niš, Faculty of Mechanical Engineering, Niš, Serbia
Dr Miloš Tasić, University of Niš, Faculty of Mechanical Engineering, Niš, Serbia
Milica Jovčevski, University of Niš, Faculty of Mechanical Engineering, Niš, Serbia
Dr Saša Pavlović, University of Niš, Faculty of Mechanical Engineering, Niš, Serbia
Dr Marko Mančić, University of Niš, Faculty of Mechanical Engineering, Niš, Serbia
Dragana Dimitrijević Jovanović, Innovation Centre of Advanced Technologies, Niš, Serbia
Dr Ivan Pavlović, University of Niš, Faculty of Mechanical Engineering, Niš, Serbia
Jovan Škundrić, University of Banja Luka, Faculty of Mechanical Engineering, Banja Luka, Republic of Srpska, Bosnia and Herzegovina
Danijela Stanisavljević, University of Niš, Faculty of Mechanical Engineering, Niš, Serbia
Jovan Milić, University of Niš, Faculty of Mechanical Engineering, Niš, Serbia
Marko Vučetić, University of Niš, Faculty of Mechanical Engineering, Niš, Serbia
Katarina Jovanović, University of Niš, Faculty of Mechanical Engineering, Niš, Serbia

Contents

The Numerical Simulation of the Friction Heat Generation on the Contact of Bodies with the Surface Roughness

***Miroslav Mijajlović*[a, CA]*, Dušan Ćirić*[b]*, Sonja Vidojković*[c]*, Jelena Mihajlović*[d]**

[a]*University of Niš, Faculty of Mechanical Engineering, Niš, RS, miroslav.mijajlovic@masfak.ni.ac.rs*
[b]*University of Niš, Faculty of Mechanical Engineering, Niš, RS, dusan.ciric@hotmail.com*
[c]*University of Belgrade, Institute of CTM, Belgrade, RS, sonja66yu@yahoo.com*
[d]*University of Niš, Faculty of Mechanical Engineering, Niš, RS, jelena.jekam93@gmail.com*

Abstract: The generation of heat, at the frictional contact of two bodies, is the most common structural-thermal process in contact engineering. As such, it has been analyzed from many different aspects and on different levels. The modern-day analysis of the frictional heat generation is usually numerical with the significant simplifications and the most common simplification in such of analysis is neglecting the surface roughness as a parameter which is slowing down the calculation process. The paper is presenting a numerical model(s) for estimation of the frictional heat but for the bodies having surface roughness included. Besides analyzing the rough-rough contact, the comparative analysis of the heat generation on the contact of the rough-flat and flat-flat bodies is done, as well. The overcome of the long-lasting calculating time is done using the small-model-shortly-loaded concept with the usage of adapted thermal boundary conditions.

Keywords: Contact, Friction, Heat Generation, Surface Roughness

1. Introduction

The frictional heat generation is a physical phenomenon always present when the contact of two bodies in the relative movement exists. While moving and contacting at the same time, from the aspect of the frictional heat generation, the bodies interact both on micro and macro levels resulting in micro and macro mechanical, frictional and thermal processes as the primary, while metallurgical, lightning, vibration, and other processes appear as the secondary [1]. Both the primary and the secondary processes involve in the energy transformation into heat. The bodies in contact carry a large amount of mechanical energy and a much smaller part of the other energy types [2]. Therefore, the phenomenon of the „frictional heat generation" is a complex mechanism of transformation of the mechanical energy into the heat at the contact interface of the bodies. The transformation is purely due to the friction and it is followed by the mechanical deformation and stressing of the bodies under the thermal (boundary) conditions. The mechanism of mechanical energy transformation into the frictional heat is, as previously mentioned, the micro and macro based and as such it can be analyzed on the micro or macro level. The engineering praxis usually prefers macro level analysis [1].

All frictional processes at the contact of two moving bodies always appear on the real contact area regardless of nominal/prescribed contact, initial and boundary conditions [1]. The prescribed (nominal) contact area is, in most of the contact cases, significantly larger than the real contact area what results in large deforming, infliction of larger stresses and fast changing of the contact configuration [3]. However, most of the materials used in the engineering have significant elasticity reserves and inert isotropic hardening which compensate by contact-induced impacts on bodies. The metallic bodies are capable to resist such hard stressing, at least for a short time period that is long enough to get the real contact area larger without significant destruction of bodies in contact. The stationary frictional contact condition is achieved when the real contact area reaches its quasi maximal value (which is almost always smaller than the nominal) [1, 3, 4].

The frictional heat generation is appearing in the real contact area due to the solid friction and the loads delivered to the contact [1]. There were serious discussions in the 1990s about the mechanisms and interfaces where the heat generation appears [1, 5, 6]. Since solid friction appears on outside interfaces of the bodies in contacts, a certain number of researches point out that the frictional heat is generated at the surfaces where the friction appears (when heat generation is considered on the macro level) [6]. In macro models, the main factors that influence heat generation are friction coefficient, frictional stresses, temperature, sliding velocity and real contact area [2, 3]. Almost all of the macro-based models point out that 95%-100% of the mechanical energy dissipated as frictional heat becomes thermal energy which is responsible for the increase of the contact body's temperatures [1, 2]. The interface friction heat is delivered to the bodies in contact in a certain ratio – when the bodies are made of the same material and have approximately the same size, this ratio is 50% to both [7, 8]. If contact bodies differ in a metallurgical, chemical or dimensional manner, the ratio of the heat distribution changes from 50-50 to some other [8]. In such a situation, the ratio is obtained experimentally [8-10]. The micro-based models assume that the frictional heat is generated on the top few atomic-layers below the contact surface but not deeper than 5μm in the bodies [5]. The micro-based frictional heat generation models consider the same mechanism for the heat generation as the macro-based models and many of them include plastic deformations of the contact surface of the contact bodies [5]. The macro-based models usually do not recognize plastic deformation and plasticity based heat generation as the frictional heat [5, 8].

The process of frictional heat generation is strongly self-regulatory [1, 2, 11]. Regardless of the initial contact pressure, temperature, sliding velocity and friction coefficient, the frictional generated heat is increasing the temperature of the bodies, at least in the contact area. When heating is intense, the increase of the body's temperature results in softening of the material, what furthermore induces a certain drop of the friction coefficient [11]. If heating of the bodies continues the material becomes even softer and the intensive drop of the friction coefficient appears. In such a circumstance, the amount of mechanical energy being transformed into the frictional heat significantly drops, as well, and the bodies in contact start to locally cool down [1, 11]. The material cooling induces the material hardening and the friction coefficient increase, what again triggers the body's temperature increase and the loop continues from the start [11]. Therefore, the frictional heat cannot melt the bodies in contact (on the macro-level) – several experimental investigations show that maximal temperature achieved by frictional heating can reach 75%-85% of the material's melting temperature [1, 11]. If wear and abrasion of the contact are not significant, the friction coefficient and contact pressure are merely depending on the temperature of the contact bodies, loads and topology [12].

The estimation of the amount of frictional generated heat can be done analytically, numerically or experimentally [1, 12]. The analytical approach is mostly used for the contact problems with the simple contact topology and the constant loading conditions. The experimental approach is based on the measuring/estimation of mechanical energy present in the contact area that is multiplied with the correlation factor – heat efficiency transformation factor. Usually, the correlation factor varies from 0.5 to 1.0 and it cannot be defined universally [1, 11-13]. The numerical approach is mostly used in the present days and it relies on analytical method an experimental data for more precise results. The numerical estimation of the heat generated due the friction requires fully coupled structural and thermal conditions, what cannot be done without discretization of the space and time and approximate solution of the frictional, deformational, stress and thermal processes. The discretization of the bodies demands to neglect many structural-topological features of the bodies in contact [10, 14, 15] while discretization of the time is influenced by the minimal dimensions of the discretized bodies and convergence requirement of the approximate solving method [13].

The easiest path for the numerical estimation of the amount of frictionally generated heat is using some commercial software that has capabilities to estimate complex mutual structural-thermal relationships of the bodies in contact. However, the main issues with such an approach are hardware limitations of the calculating machines – the relatively small numerical models and relatively short termed contact processes require significant computational resources and long-lasting processing time. Many of the numerical frictional heat generation models neglect the contact surface roughness, hardness and time/temperature dependent properties of the bodies or contact [16-27]. This paper is dealing with the contact frictional heating of the bodies having surface roughness involved in the numerical model ran by Ansys Workbench coupled transient structural-thermal solver.

2. The Problem Formulation and the Model

The frictional heat generation has been considered for the contact of 2 bodies in 3 cases: in the 1st case is considered the contact of 2 ideally flat bodies (Figure 1, a), the 2nd case is dealing with the contact of a flat fixated body and a rough moving body (Figure 1, b) and the 3rd case analyses the contact of 2 rough contact bodies (Figure 1, c).

The surface roughness of the contact surfaces on the bodies is modeled in a manner to be comparable to the

ISO 4287: Geometrical Product Specifications (GPS) – Surface texture: Profile method – Terms, definitions, and surface texture parameters [28]. The flat contact surfaces have no surface roughens and they satisfy the N0 surface quality (R_a=0 μm) while the rough contact surfaces comply with the N6 surface quality (R_a=0.8 μm).

The basic geometrical models used for the contact/friction heat generation analysis are rather small (the moving body is 0.1 mm × 0.1 mm × 0.05mm and the fixed body is 0.22 mm × 0.12 mm × 0.02 mm) and the highest peaks/deepest valleys of the surface roughness are 5 μm. Entering into the micro-unit dimensions in the frictional heat generation numerical analysis demands a great number of small discretized elements, what furthermore requires a significant number of structural and field equations to be solved, using a small time step (app. 10^{-6} s to 10^{-4} s) to achieve convergence. This requires significant computational time and hardware resources and these are the main reasons why the dimensions of the bodies need to be small.

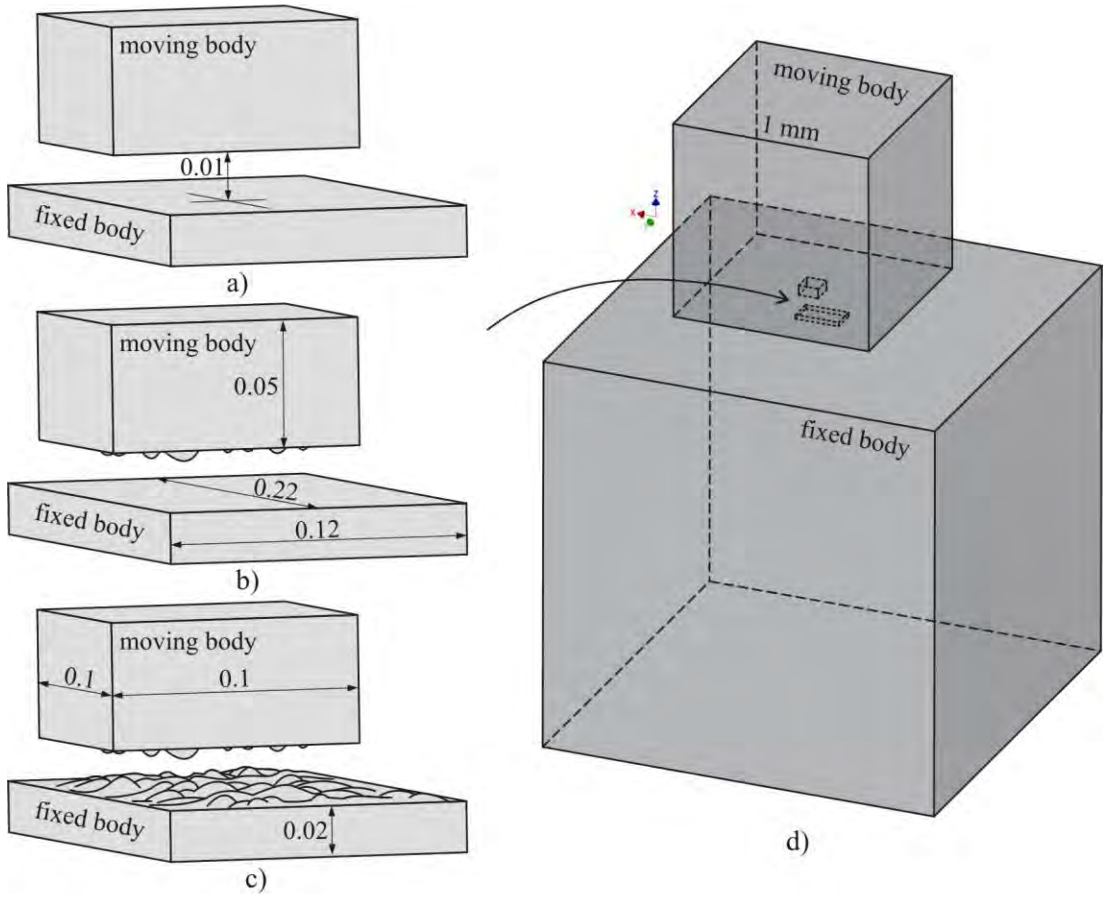

Figure 1. The models (in mm) used for the frictional heat generation for a) flat-flat contact, b) rough-flat contact, c) rough-rough contact, d) enlarged model for thermal analysis

On the other hand, setting up the conventional thermal boundary conditions (convection, conduction), the body heating (heat transport within the body) and the heat transfer from a body to a body (conduction, radiation) on such a small body cannot be modeled in a fully realistic manner – there are no (or: there are a few specific) engineering parts so tiny but suffering heavy frictional-thermal loadings like the planned models are about to. The model has to be significantly larger. Fortunately, pure thermal modeling is less sensitive to the time step size and size of the discretized elements than combined (coupled) structural-thermal modeling, and this gives a possibility to create another, larger model of the bodies in contact (having dimensions of max. 2 mm × 2 mm × 2 mm, shown in Figure 2, d), which embeds the small model inside itself. In such of a configuration, there is no physical separation between the bodies (the structure is monolith), but there is a geometrical boundary between the small and enlarged model where the adapted thermal boundary conditions for the small model can be defined. This is modeled using the thermal flux passing thru the geometrical boundary and the procedure will be given in the following chapters.

Initially, the bodies are positioned one above the other at the distance of 0.01 mm from the nominal contact surfaces of the bodies. The nominal contact surfaces are the surfaces planned to get into contact with N0 roughness for the flat bodies and „0-surfaces” for the N6 roughness surfaces [28]. The nominal surface has a nominal contact area of A_n=0.1 mm·0.1 mm=0.01 mm^2. During the first 0.01 s the moving body is coming down to the fixed body, traveling 0.01 mm. During this time, the bodies get in contact. Afterward, the moving body travels in the direction along the longer edge of the fixed body passing 0.1 mm in 0.1 s, staying in contact with the fixed body. At the end of the cycle, the moving body is traveling upwards for 0.01 s traveling 0.01 mm, leaving the contact with the fixed body. In total, the complete cycle lasts for 0.12 s.

2. The Numerical Model and Simulation

The problem is simulated and analyzed using The Ansys Workbench as a coupled structural-thermal analysis combined with the transient thermal analysis (Figure 2). The simulation for all of the 3 cases is done in 3 steps. Step 1 is a coupled structural-thermal numerical analysis of the small (base) model without the thermal boundary conditions and without the conduction between the bodies. The main goal is to estimate the amount of generated frictional heat delivered to the bodies in contact (as the heat flux in W/m^2). The heat flux from Step 1 is used as an input value in the pure transient thermal analysis done in Step 2. In this step, the used model is enlarged and it is used for estimation of the heat flux transportation thru the base model's boundary surfaces and temperature distribution thru the bodies. The estimated flux on the boundaries of the small body is used for estimation of the adapted convection coefficients (Figure 3) that are necessary for more precise estimation of the heat generated due to the friction on contact in Step 3. Step 3 is structurally the same as Step 1 but it uses adapted convection coefficients on boundary surfaces, conduction between the bodies in contact and the temperature dependent coefficient of friction (Figure 3). The generated heat on the contact and the temperature of the bodies are the main results from the step 3.

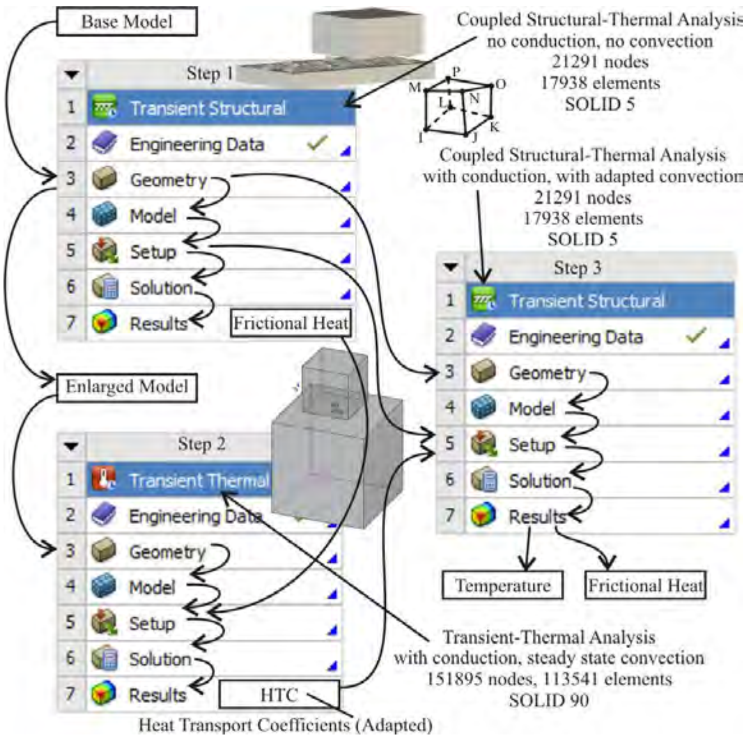

Figure 2. The schematic of the Ansys Workbench numerical simulation with some details about the numerical models

The numerical model in Steps 1/3 (coupled structural thermal analysis) is based on the base model and it is discretized with 17938 linear SOLID 5 elements [29]. The numerical model in Step 2 (transient thermal analysis) is based on the enlarged model and it is discretized with 113541 SOLID 90 elements [30].

The heat generation due the friction is modeled under assumptions that the bodies in contact are ideally elastic, isotropic, the complete mechanical energy on the contact is transformed into the heat and the heat is equally distributed to both bodies in contact. The friction coefficient is assumed to be temperature dependent only $\mu(T)$. The temperature T is an average temperature of the contact surface. Both bodies are made of structural steel (Figure 3). The radiation, surface hardness, wear, adhesion, fatigue, creep and surface hardening are not considered in the numerical simulation.

The frictional heat flux generated on the contact (the rate of frictional dissipation) at the node *i* at the time moment of *t* $q_i(t)$, is estimated as (Equation 1):

$$q_i(t) = FHTG \cdot \tau_i(t) \cdot v_i(t) \tag{1}$$

The frictional dissipated energy converted into heat is considered to be 100 % as a general assumption. It is defined as a 15th real constant in Ansys MAPDL with a value of FHTG=1.00.

The equivalent frictional stress at the node *i* at the time moment of *t* $\tau_i(t)$ is estimated using Coulomb's law of friction and it is a function of the coefficient of friction and the contact pressure in the node *i* (Equation 2):

$$\tau_i(t) = f\left[\mu(T), p_i(t)\right] \tag{2}$$

The contact pressure at the node *i* at the time moment of *t* $p_i(t)$ is determined by the software's solver and it is influenced by the contact conditions and the loading of the bodies. The sliding rate at the node *i* at the time moment of *t* $v_i(t)$ is estimated by the software's solver as a contact-dependent variable.

The distribution of frictional heat to the bodies in contact is defined with the weight factor for the distribution of heat between the bodies in contact and it is assumed that each body gets 50% of the generated heat. It is defined as an 18th real constant in Ansys MAPDL with a value of FWGT=0.50.

The conduction between the elements in the contact is defined over the heat flux $q_{cond}(t)$ delivered from the hotter element (temperature T_{hot}) to the colder element (temperature T_{cold}) (Equation 3):

$$q_{\mathrm{cond}}(t) = TCC \cdot \left(T_{hot} - T_{cold}\right) \tag{3}$$

The thermal contact conductance coefficient (TCC) is a material and contact property indicating thermal conductivity-heat conduction between bodies in contact. It is a phenomenon defined by many factors where the main factors are contact pressure, contact area, surface deformation, metallurgical parameters and the cleanness of the surfaces in contact. The problem of TCC estimation is too complex to be analyzed here – it is usually estimated experimentally but there are many works trying to find an analytical solution [22]. Assuming minor heating during the contact, for simplification, the TCC is taken to be constant TCC=50 $\mathrm{kW\cdot m^{-2}\cdot °C^{-1}}$. The convection at the free-air surfaces is considered to be constant h=10 $\mathrm{W\cdot m^{-2}\cdot °C^{-1}}$. For the surfaces of the base model which are the geometrical boundaries in the enlarged model (and free-air in the base model), during step 2 the heat flux traveling thru the surface has been estimated. For example, for the surface at the moving body in –*x*-direction, the equilibrium equations are (Equations 4 and 5):

$$\text{for the base model } q_{-x}(t) = -h_{ad\,x}(t) \cdot \left[T_0 - T(yz,t)\right] \tag{4}$$

$$\text{for the enlarged model } q_{-x}(t) = k \left.\frac{dT(yz,t)}{dx}\right|_{-x} \tag{5}$$

The adapted coefficient of convection in –*x*-direction $h_{ad\,x}(t)$ is (Equation 6):

$$h_{ad\,x}(t) = -\frac{q_{-x}(t)}{T_0 - T(yz,t)} \tag{6}$$

It is much more appropriate having adapted coefficient as a function of the average temperature at the surface and the prescribed heat flux thru the surface (Equation 7):

$$h_{ad\,x}(T) = \frac{q_{-x}}{T_{a\,yz} - T_0} \tag{7}$$

Finally, establishing the connection between the total generated frictional heat, generated at the contact surface (Equation 8):

$$q_v(t) = \sum_{i=1}^{i=n} q_i(t) \tag{8}$$

and the average heat flux traveling thru the boundary surfaces of the base model within the enlarged model (q_x, q_y, q_z) the adapted coefficients of the convection for the free surfaces at the base model used in Step 3 are defined as (Equations 9 to 11):

$$h_{ad\,x}\left(q_v,T,t\right)\approx-\frac{q_x\left(q_v,yz\right)}{T_\infty-T\left(yz,t-\Delta t\right)}\tag{9}$$

$$h_{ad\,y}\left(q_v,T,t\right)\approx-\frac{q_y\left(q_v,xz\right)}{T_\infty-T\left(xz,t-\Delta t\right)}\tag{10}$$

$$h_{ad\,z}\left(q_v,T,t\right)\approx-\frac{q_z\left(q_v,xy\right)}{T_\infty-T\left(xy,t-\Delta t\right)}\tag{11}$$

The solver estimates total generated frictional heat, uses average temperatures (from the previous time step) of the observed surface for which adapted coefficients are estimated for then uses the equations to estimate the adapted coefficients for every time step. Figure 3 shows the most important details for understanding the problem. The environment temperature is T_0= T_∞=22°C.

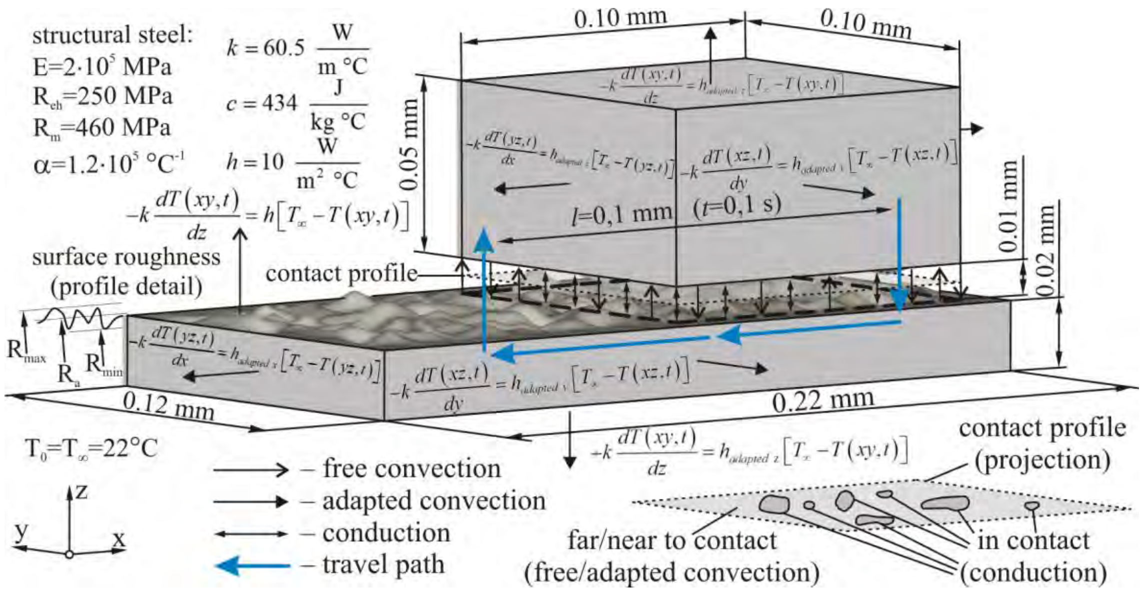

Figure 3. The base model showing base dimensions, prescribed boundary conditions, contact status, and some material properties of the bodies in step 3 on the rough-rough model setup

3. The Simulation Results

The contact of the flat-flat bodies initiates simultaneously at all contact points at the time of 0.01 s – when moving body stops translating downwards. The real contact area between the bodies (A_r) is equal to the nominal contact area (the ratio is A_r/A_n=100%). For the rough-flat and rough-rough bodies, the initial contact happens before 0.01 s – the moving body is translating downwards but the highest peaks on the moving/fixated body get in contact with the opposite side element. The real contact area, in both cases, enlarges until the translation of the moving body stops. However, at that moment the real contact area is smaller than the nominal (the ratio is A_r/A_n =65%-70%). When translation – sliding of the moving body over the fixated body starts (at 0.01 s), the ratio A_r/A_n drops to app 43%-45% for the rough-flat body contact while ratio A_r/A_n oscillates between 30%-50% for the rough-rough contact. For the flat-flat contact, the ratio remains 100% (Figure 4). When moving body start translating away from the fixed body (after 0.11 s), the contact area between the bodies fast changes from its previous value to significantly smaller values and therefore the ratio A_r/A_n fast reaches the values of 0 for all body configurations. The areas in contact (sliding and sticking) are the locations where the frictional heat generates and conduction between the moving and fixated body appears (Figures 5 to 7). The remaining area in the contact region with near-to contact and far-away from contact statuses have convective boundary conditions. Step 1 had a goal to estimate the amount of heat generated in contact (Figure 8). The exchange of the heat between moving and fixated body was disabled – there was no conduction, convection or radiation between the bodies in contact. The heat exchange on the other boundary surfaces of the bodies was disabled as well. The result of such heat transportation restrictions are the unrealistic high temperatures of max. 35 °C (rough-flat) / 66 °C (rough-rough) at the moving body.

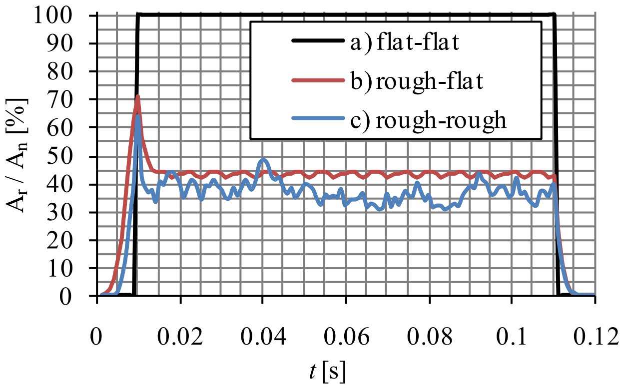

Figure 4. The ratio between the real and nominal contact area

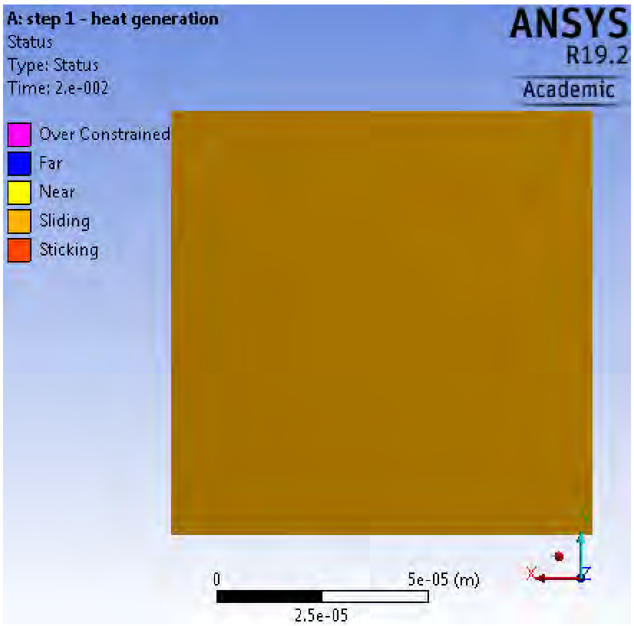

Figure 5. The contact status for the flat-flat

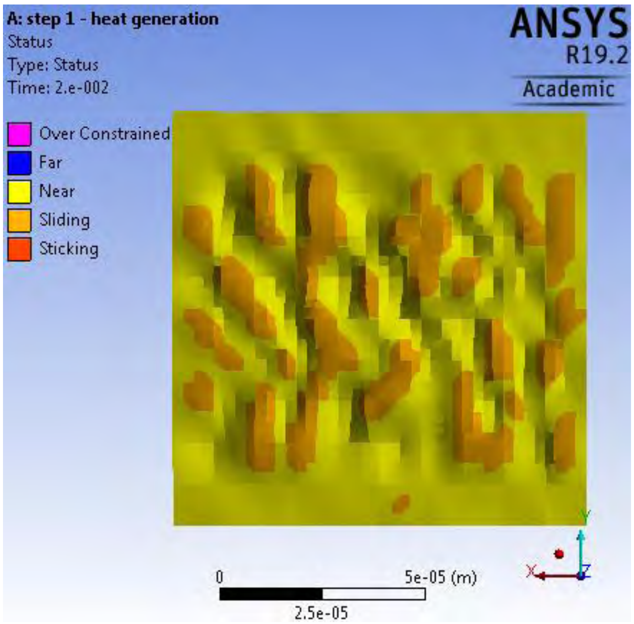

Figure 6. The contact status for the rough-flat

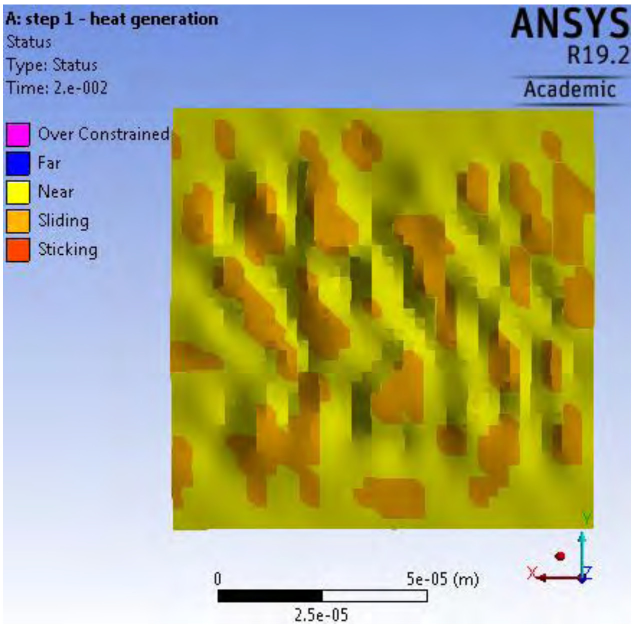

Figure 7. The contact status for the rough-rough

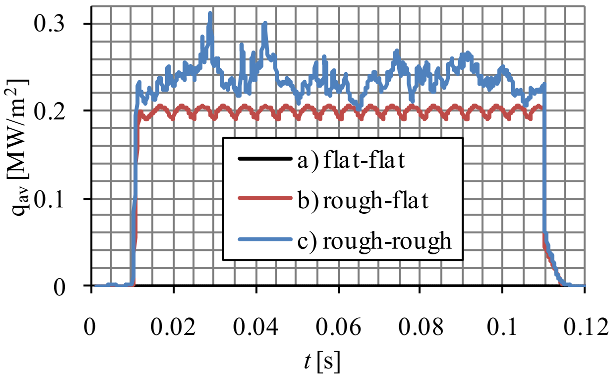

Figure 8. The average frictional generated heat

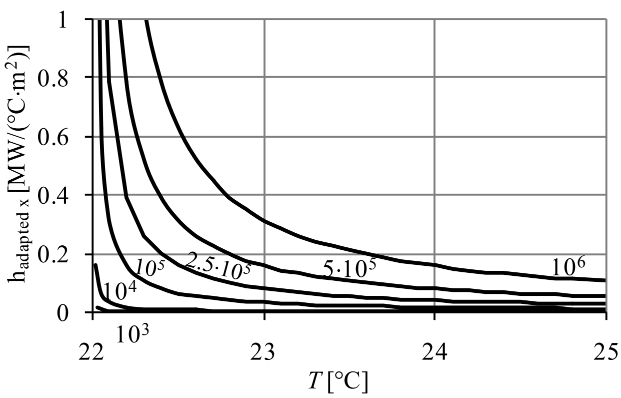

Figure 9. The adapted convection coefficient for x-direction surfaces

Prilog 18

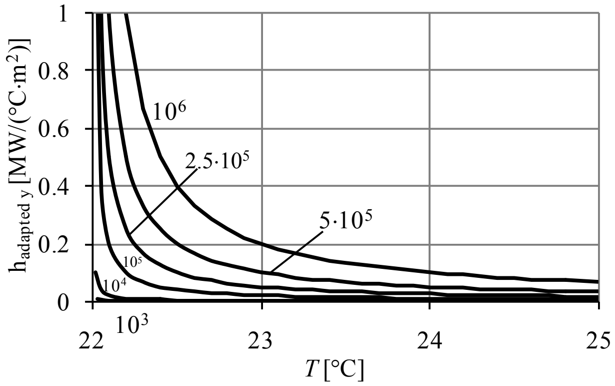

Figure 10. The adapted convection coefficient for y-direction surfaces

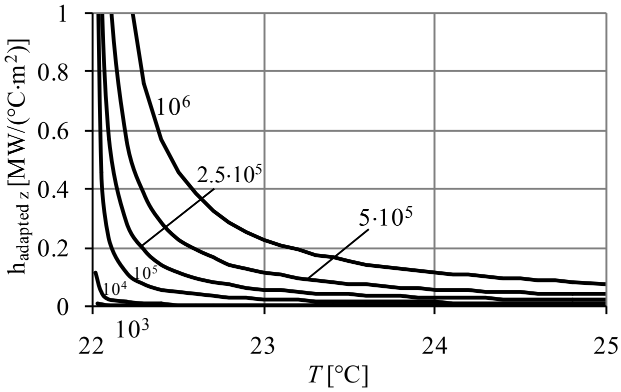

Figure 11. The adapted convection coefficient for z-direction surfaces

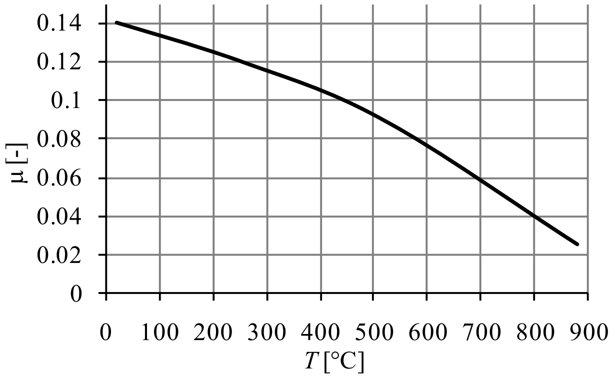

Figure 12. The temperature dependent friction coefficient

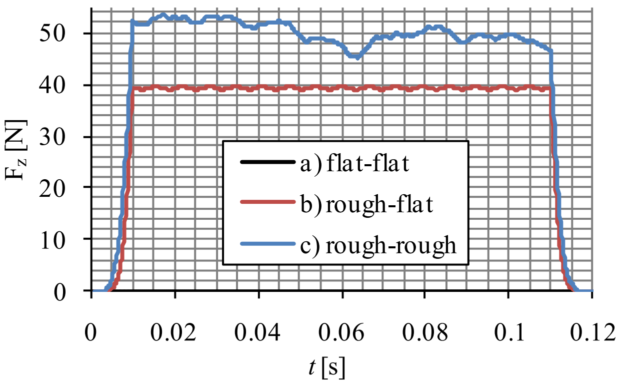

Figure 13. The force reaction in z-direction

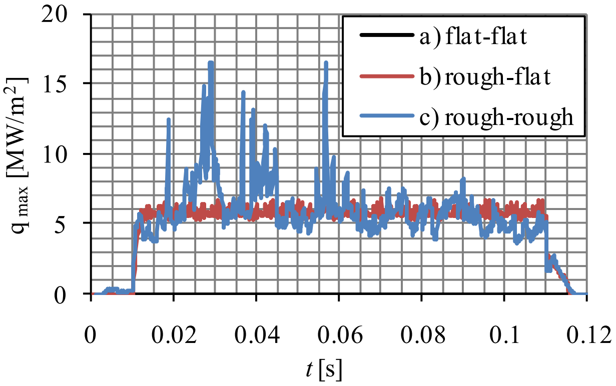

Figure 14. The max. values of the generated frictional heat

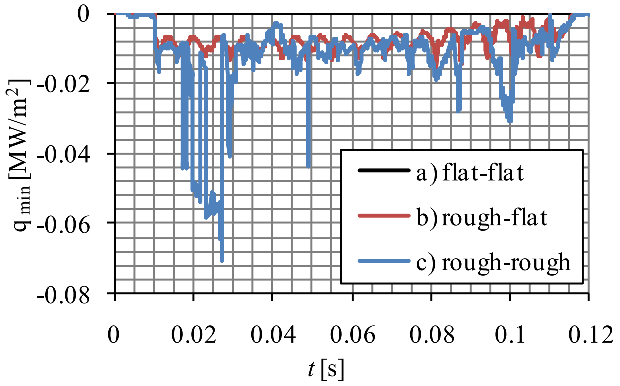

Figure 15. The min. values of the generated frictional heat

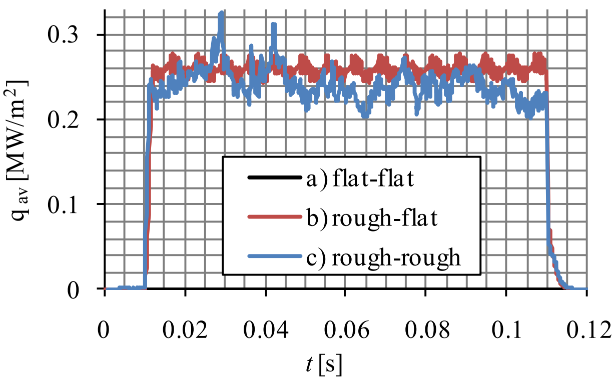

Figure 16. The average values of the generated frictional heat

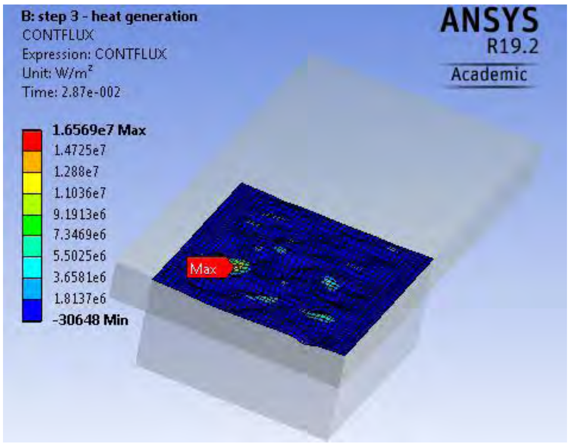

Figure 17. The extreme value of the generated frictional heat at the rough-rough contact

The frictional generated heat from Step 1 (Figure 8) is used as an input heat flux for Step 2 where the enlarged model is used. The main results from Step 2 are the functional dependencies between the frictional generated heat, heat flux leaving the base model and the average temperature (Figures 9 to 11). Step 3 uses an algorithm for estimation of adapted convection coefficients based on the frictional heat generated on the contact and temperature of the considered element. The friction coefficient on the contact in Steps 2 and 3 is considered to be temperature dependent (Figure 12).

The complete model analyzed in Step 3 gave all results: the force reaction F_z (Figure 13), the generated frictional heat (Figures 14 to 17), temperature (Figures 18 and 20) and contact pressure (Figure 21).

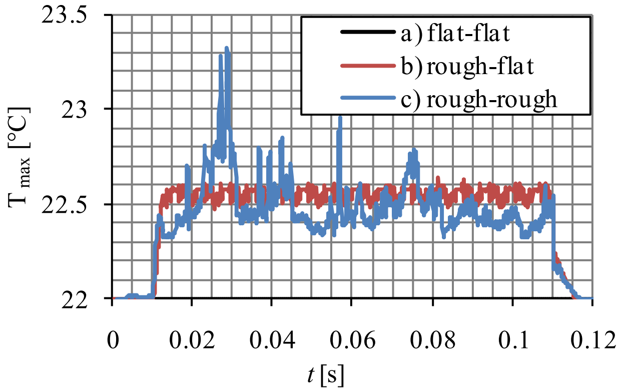

Figure 18. The maximal values of temperatures

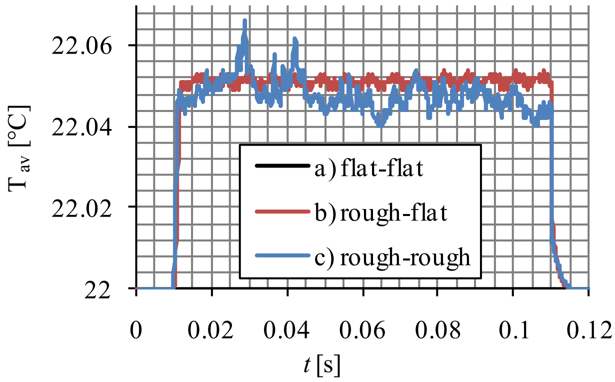

Figure 19. The maximal values of temperatures

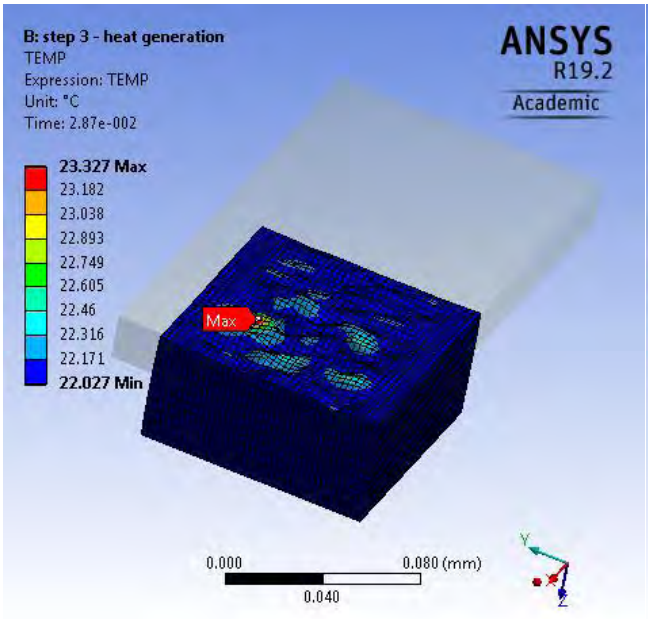

Figure 20. The extreme value of the temperature at the rough-rough contact

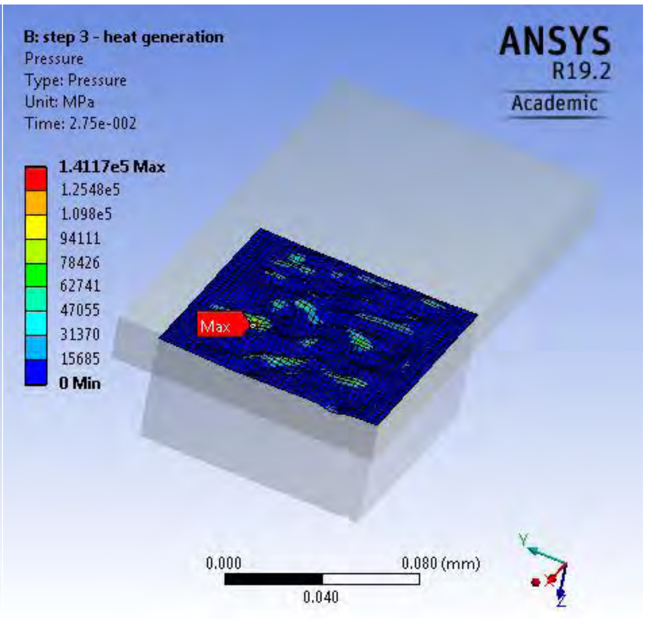

Figure 21. The extreme value of the contact pressure at the rough-rough contact

3. Discussion and Conclusions

The frictional contact and frictional heat generation that involves surface roughness is a challenging task to deal with due to several reasons. The surface roughness in metallic real bodies is dimensioned in micro-length units while the real bodies are mostly in mili-length units. Therefore, the discretized model of such bodies must have a large number of small elements that will give a satisfactory representation of the surface roughness and processes that appear on contact. Finally, the numerical stability of the transient structural simulation, when small elements are applied, can be achieved only if the small time step is applied. It is obvious that a powerful calculating system is needed, working for a long time period.

The reasonable solution is to use small bodies (small model), consider it as a large body and surround it with the boundary conditions that represent a large body in a process lasting for a short time period (short time process). Such an approach delivers good frictional, contact and thermal results but some of the structural results might be ambiguous (for example stresses) due to the compromised stiffness of the bodies.

Using the small model approach, the frictional contact is analyzed for 3 cases: flat surface to flat surface, rough surface to flat surface and rough surface to rough surface. The bodies have been initiated to touch over the prescribed surfaces until the nominal surfaces come to touch. For such a condition, flat-flat contact initiates near to 0 (the numerical tolerance level of 10^{-8} units) resistance force, no frictional heat flux, no contact pressure and no heating of the bodies. The frictional heat generation and the temperature increase are possible only if the flat bodies get more „pressed" one to another. Anyhow, the real contact area of the bodies is equal to the nominal contact area what is not the case for the real bodies having surface roughness.

The moving body from the rough-flat contact initiates contact with the fixed body at 0.0048 s what is much earlier than the nominal contact surfaces touch each other for the flat-flat contact (at 0.01 s) At that moment, the highest peak of the surface roughness on moving body touches the flat surface of the fixed (flat) body and the heat transportation between the bodies begins – the heat generation and distribution to both bodies, as well as the conduction from the hotter body to the colder body over the estimated real contact area. The conduction is modeled as constant, regardless of time, contact area, contact pressure or temperature, what it certainly is not in reality. It is assumed to be constant value to relax the numerical calculation and under the assumption that the complete loading cycle lasts very short. This should be investigated in further researches. The real contact area increases up to maximal 71% of the nominal contact area at the end of the downward translation of the moving body. When the moving body starts to translate over the fixating body, the real contact area varies from 40% to 50% of the nominal contact area. This decrease of the real contact area is induced by the change of the contact status from sticking to sliding: the elements in contact start to relatively move one compared to another what decreases active contact between them. The elements in sliding condition generate an average heat flux delivered to each body from 0.24 MW/m^2 to 0.28 MW/m^2. The maximal heat flux delivered to elements at the highest peak of the surface roughness is 6.84 MW/m^2 while the element that is not in the contact, located in the deepest valley of the surface roughness, delivers to the surrounding maximally 0.007 MW/m^2 over convection. These short bursts of energy in contact areas do not significantly change the temperature of bodies in contact – the maximal temperature is 22.64 °C, in the zone of the highest peak on the surface roughness. The average temperature of the bodies varies from the 22.044 °C to 22.048 °C. The moving body from the rough-rough contact, initiates contact even earlier, at 0.0032 s, when one of the surface roughness peaks at the moving body initiates contact with some surface roughness peak at the fixating body. From that point forward, the real contact area increases to maximal 65% of the nominal contact area. When the moving body starts translation along the fixated body, the real contact area drops down and oscillates from 30% to 50% of the nominal value. This variation is the product of initiation of new contact points as well as the breakage of the previously initiated contacts. The average generated flux delivered to each body is between 0.20 MW/m^2 to 0.35 MW/m^2. The maximal generated heat flux delivered to the bodies is 16.8 MW/m^2 and it appeared at the contact of two high peaks. The maximal heat flux delivered to the surrounding is 0.07 MW/m^2 at the location on top of a small valley on the fixated body. Slightly larger average heat flux generated on the rough-rough contact than heat flux generated on the rough-flat contact results in a slightly higher average temperature of the bodies – from 22.04 °C to 22.068 °C. The maximal temperature for the rough-rough contact is higher than for the rough-flat contact – at the location where the maximal heat flux has been generated, the maximal temperature has reached 23.327 °C.

Clearly, the rough-rough contact initiates higher peaks in the heat generation due to the higher contact pressures between the two high roughness surface peaks. In simulated case, the highest contact pressure for the rough-rough contact is 141.170 GPa while expected nominal contact pressure is for the axial force of 50 N equal to the 5 GPa. The larger model and the longer frictional contact between the rough-rough bodies would result in more locations where extreme values of the frictional heat would appear. This will lead to more intensive heating than for the flat-flat contact or the rough-flat contact.

The more detailed investigation of the surface roughness influence to the frictional heat generation in numerical research has to be done. It is necessary to estimate the cost-benefit: comparing the calculation time and the hardware resources engaged for the more precise results. At the present state of calculation technique, it seems to be ineffective using surface roughness in simulating frictional heat generation – the simulation would last too long and the precision of the results would not be dramatically better than results gathered in simulations without surface roughness involved. The future models should involve wear, non-linear deforming, plasticity, but that would slow down the simulations even more.

The coupled structural-thermal analysis is done using SOLID 5 linear hexagonal elements with the limited coupling abilities [29]. The SOLID 5 element is a „legacy element" of the Ansys software from the end of the 20th century and Ansys Workbench recommends the usage of the current, fully-coupling, newer and more advanced SOLID 226 element [31]. However, SOLID 226 elements have shown instability concerning the temperature estimation while frictional heating. There are many published examples where the frictional heating appears but the bodies show temperature decrease (cooling below the ambient temperature) [23-27]. The same situation has appeared during testing of the presented numerical models with SOLID 226 elements. Therefore, authors have decided to use proven, limited but functional, non-state-of-the art technology. The authors have several times addressed this issue to the Ansys Customer Service but no response has happened until the finalization of this research.

Nomenclature

Latin symbols

A_n	–Nominal contact area, in [mm^2].
A_r	–Real contact area, in [mm^2].
F_z	–Force reaction in z dir., in [N].
$FHTG$	–Fraction of frictional dissipated energy converted into heat.
$FWGT$	–Weight factor for the distribution of heat between bodies.
$p_i(t)$	–Contact pressure at the node i at the time moment of t, in [MPa].
$v_i(t)$	–Sliding rate at the node i, in [m·s^{-1}].
R_{eh}	–Tensile yield strength, in [MPa].
R_m	–Ultimate yield strength, in [MPa].
E	–Young's modulus of elasticity, in [MPa].
R_a	–Arithmetic average of the roughness profile, in [μm].
i	–Node counter.
t	–Time, in [s].
T	–Temperature, in [°C].
$T_0,\ T_\infty$	–Environment temperature, in [°C].
$T_{a\,yz}$	–Average temperature at the yz boundary surface, in [°C].
$T(yz,t)$	–Temperature at the yz boundary surface, in [°C].
$T(xy,t-\Delta t)$	–Temperature at the xy surface, at the previous time step, in [°C].
$T(xz,t-\Delta t)$	–Temperature at the xz surface, at the previous time step, in [°C].
$T(yz,t-\Delta t)$	–Temperature at the yz surface, at the previous time step, in [°C].
T_{hot}	–Average temperature of the hotter contact surface, in [°C].
T_{cold}	–Average temperature of the colder contact surface, in [°C].
TCC	–Thermal contact conductance coefficient, in [W·m^{-2}·°C].
c	–Specific heat capacity, in [Jkg^{-1}°C^{-1}].
k	–Thermal conductivity, in [Wm^{-1}°C^{-1}].
l	–Travel distance, in [mm].
$h_{air},\ h$	–Thermal convection coefficient surface to air, in [W·m^{-2}·°C].
$h_{ad\,x}(t)$	–Adapted thermal con. coefficient for x surface, in [W·m^{-2}·°C].
$h_{ad\,y}(t)$	–Adapted thermal convection coefficient for y dir., in [W·m^{-2}·°C].
$h_{ad\,z}(t)$	–Adapted thermal convection coefficient for z dir., in [W·m^{-2}·°C].
$h_{ad\,x}(q_v,T,t)$	–Adapted thermal conv. coefficient for x dir., in [W·m^{-2}·°C].
$h_{ad\,y}(q_v,T,t)$	–Adapted thermal conv. coefficient surface for y v, in [W·m^{-2}·°C].
$h_{ad\,z}(q_v,T,t)$	–Adapted thermal conv. coefficient surface for z dir., in [W·m^{-2}·°C].
$q_i(t)$	–Frictional heat flux generated on the contact, in [W·m^{-2}].
$q_{cond}(t)$	–Frictional heat flux delivered by conduction on contact, in [W·m^{-2}].
$q_v(t)$	–Total generated frictional heat at the contact surface, in [W·m^{-2}].
$q_{-x}(t)$	–Frictional heat flux passing thru –x surface, in [W·m^{-2}].
$q_x(q_v,yz)$	–Frictional heat flux passing thru x surface, in [W·m^{-2}].

$q_y(q_v, xz)$ –Frictional heat flux passing thru y surface, in [W·m^{-2}].

$q_z(q_v, xy)$ –Frictional heat flux passing thru z surface, in [W·m^{-2}].

Greek symbols

α –Coefficient of linear thermal expansion, in [°C^{-1}].

$\mu(T)$ –Temperature dependent coefficient of friction, in [-].

$\tau_i(t)$ –Equivalent frictional stress at the node i at the time t, in [MPa].

Δt –Time step, in [s].

References

[1] Djurdjanovic, M., Stamenkovic, D: Tribologija presovanih spojeva: monografija, Nis, 2005

[2] Kennedy, F. E., Frictional Heating and Contact Temperatures, in: Modern Tribology Handbook (Bharat Bhushan), CRC Press LLC, Boc Ratona, 2001, Chapter 6

[3] Fortunato, G. et al: General Theory of Frictional Heating with Application to Rubber Friction, J. Phys. Condens. Matter, 27 (2015), pp. 1-16

[4] Djurdjanović, M. et al, Heat Generation During FSW Process, Trib. in Ind., 31 (2009), 1-2, pp. 8-14

[5] Landman, U., Luedtke, W.D., Ringer, E.M., Molecular dynamics simulations of adhesive contact formation and friction, in Fundamentals of Friction: Macroscopic and Microscopic Processes, Singer, I.L., Pollock, H.M. (Eds.), Kluwer Academic Publishers, Dordrecht, 1993, pp. 463

[6] Kennedy, F.E., Frusescu, D., and Li, J. (1997), Thin film thermocouple arrays for sliding surface temperature measurement, Wear, 207 (1997), 1, pp. 46-54

[7] ***, ANSYS theory manual, Ansys Contact Technology Guide, SASIP. INC, 2004,

[8] Milošević, M. et al, Distribution of Generated Friction Heat at Wheel-Rail Contact During Wheel Slipping Acceleration, Thermal Science, 20-5 (2016), pp. S1561-1571

[9] Kennedy, C. et al, Transient Heat Partition Factor for a Sliding Railcar Wheel, Wear, 261(2006), 7, pp. 932-936

[10] Miltenović, A. et al, Determination of Friction Heat Generation in Wheel-Rail Contact Using FEM, Facta Universitatis Series: Mechanical Engineering, 13 (2015), 2, pp. 99-108

[11] Mijajlović, M., Research and Development of an Analytical Model for Estimating the Amount of Heat Generated During Friction Stir Welding, Ph.D. thesis, University of Nis, Serbia, 2012

[12] Bowden, F.P., Tabor, D., Friction – An Introduction to Tribology, Anchor Press / Doubleday, Reprinted 1982, Krieger Publishing Co., Malabar 1973

[13] Isachenko, V.P., et al, Heat Transfer, University Press of the Pacific, 2000

[14] Abdullah, O.I., Effect of Surface Roughness on the Thermoelastic Behavior of Friction Clutches, FME Transactions, 43 (2015), pp. 241-248

[15] Popov, V.L., Willert, E., Hess, M., Method of Dimensionality Reduction in Contact Mechanics and Friction: A User's Handbook. III. Viscoelastic Contacts, Facta Universitatis: Mech. Engineering, 16 (2018), pp. 99-113

[16] Abdullah, O.I., Schlattmann, J., An Investigation of Heat Generation Due To Friction Using Finite Element Method, SAE International, 1 (2014), pp. 148-155

[17] Ştefancu, A.I., Melenciuc, S.C., Budescu, M., Finite Element Analysis of Frictional Contacts, The Bulletin of the Polytechnic Institute of Jassy, Construction. Architecture Section, 14 (2011), pp. 131-139

[18] Rajan, S.P. et al, An Investigation on Thermal and Friction Effect Produced by Friction Welding of SA 213 Tube to SA 387 Tube Plate, Alex. Eng. Journ, 55 (2016), pp. 101-112

[19] Mishra, A., Sharma A.K., Analysis of Heat Generation During Friction Stir Processing of Aluminium Similar Joints. J Adv Res Mech Engi Tech, 4 (2017), pp. 3-8

[20] Qureshi, P., Prajapati, A., Modeling of Rough Surface and Contact Simulation, IJSRD, 1 (2013), pp. 791-797

[21] Thompson, M., Methods for Generating Rough Surfaces in ANSYS, Proceedings, International ANSYS Users Conference & Exhibition, Pittsburgh, USA, March 2006.

[22] Chadouli, R., Makhlouf, M., Modeling of the Thermal Contact Resistance of a Solid-Solid Contact, IOSR, 11 (2014), pp. 72-82

[23] https://www.youtube.com/watch?v=_hrZVJg8b3o, (07.05.2019)

[24] https://www.youtube.com/watch?v=SD01heOgvrQ&t=2s, (07.05.2019)

[25] https://www.youtube.com/watch?v=ibe4Ncgm-ko, (07.05.2019)

[26] https://www.youtube.com/watch?v=6_EIp1Qz_pU, (07.05.2019)

[27] https://www.youtube.com/watch?v=31n0AtdP7K4, (07.05.2019)

[28] ISO 4287: Geometrical Product Specifications – Surface texture: Profile method – Terms, definitions and surface texture parameters

[29] https://www.sharcnet.ca/Software/Ansys/16.2.3/en-us/help/ans_elem/Hlp_E_SOLID5.html, (07.05.2019)

[30] https://www.sharcnet.ca/Software/Ansys/17.0/en-us/help/ans_elem/Hlp_E_SOLID90.html, (07.05.2019)

[31] https://www.sharcnet.ca/Software/Ansys/16.2.3/en-us/help/ans_elem/Hlp_E_SOLID226.html, (07.05.2019)